

# Functional Bases of the Spatial Dispersal of Venom during Cobra “Spitting”<sup>\*</sup>

Bruce A. Young<sup>1,†</sup>

Melissa Boetig<sup>1</sup>

Guido Westhoff<sup>2</sup>

<sup>1</sup>Department of Biology, Washburn University, Topeka, Kansas 66621; <sup>2</sup>Institute of Zoology, University of Bonn, Poppelsdorfer Schloss, 53115 Bonn, Germany

Accepted 7/11/2008; Electronically Published 12/1/2008

## ABSTRACT

Spitting cobras expulse venom toward the face and/or eyes of potential predators as part of their defensive repertoire. Evaluating the accuracy of the cobras is difficult because the spit venom does not land as a point but rather is distributed, in some cases widely, in complex geometric patterns on the surface of the target. The purpose of this study was to explore the functional bases of the venom’s spatial distribution. Using a combination of spatial analysis of “caught” venom, morphology, high-speed digital videography, and electromyography (EMG), three hypothesis were evaluated. Two of these hypotheses—that the spatial distribution was due to differential venom pressure produced by the contractile activity of the adductor mandibulae externus superficiali and that the spatial distribution was produced by the morphology of the venom canal within the fang—were both rejected. The third hypothesis—that the spatial distribution was due to rapid rotational movements of the head about the vertebral column—was supported by analyses of EMG activity within the cervical axial muscles and by predictions of venom-distribution patterns based on these cephalic displacements. These results suggest that the ability to “spit” venom is a unique suite of specializations involving both the axial and the cephalic systems.

## Introduction

Myths and old natural history texts contain reports of serpents capable of ejecting venom, fire, or other caustic substances (e.g.,

Warmington’s 1942 edition of Pliny’s *Natural History*). While many of these accounts are too fanciful to relate to extant species, others can be credibly associated with African and Asian cobras (see Alexander 1963). Laurenti (1768) provided the first formal definition of a spitting cobra (*Naja siamensis*)—the earlier definitions of cobras proffered by Linnaeus were all of nonspitting forms—and several other spitting species were described during the early 1800s. Despite the taxonomic recognition of these species, there remained considerable uncertainty regarding many aspects of the “spitting” behavior.

Gadow (1901, p. 632) wrote that “the name Spy-Slange, meaning Spitting Snake, refers to the habit which this and other African Cobras have of letting the poison drop from the mouth like saliva when they are excited. This is not a particularly economical habit, nor is it of the slightest use to the snake.” The year before Gadow’s work was published, Jones (1900) published a note titled “Can a cobra eject its venom?” To his credit, Jones answered in the affirmative, and provided a clear account of venom “spitting.” In the early 1900s a number of major works detailed Asian and African herpetology (e.g., FitzSimons 1912; Wall 1921; Smith 1943), all with descriptions of venom spitting by cobras, albeit with some uncertainties about the mechanics and nature of the fluid being spit.

Bogert (1943) provided the most detailed description of the spitting behavior and documented the dentitional specializations that enable the cobra to propel its venom forward. Despite the detail in Bogert’s contribution, several questions remained unanswered. Ditmars (1931) described how skeletal muscle acting on the venom gland would produce the motive force for the venom; Bogert (1943) cited Wall’s (1921) description of the cobra’s venom gland in support of Ditmars’s view. Interestingly enough, however, Wall (1921, p. 466) stated, “I believe the venom ejected is shaken off the fangs, and carried forward by the vehemence of the thrust. In some instances, however, where a shower of spray is reported it is more probably caused by the explosive expiratory blasts from the glottis.” Subsequent workers (e.g., Broadley 1972; Visser and Chapman 1978) continued to discuss exhaled airstreams and forward lunging as propulsive mechanisms for the spit venom. These alternative methods were explored and rejected through observations and simple behavioral experiments by Rasmussen et al. (1995). The role of the skeletal muscle in propelling the venom was demonstrated by Freyvogel and Honegger (1965), and Young et al. (2004) used a variety of experimental approaches to document the functional basis of venom spitting.

Bogert’s (1943) treatise is full of direct and secondhand descriptions of spitting cobras directing the venom at the eyes of their targets. Barbour (1922) explicitly assumed that a cobra could recognize and accurately target the eyes of a potential

<sup>\*</sup> This paper was a contribution to the symposium “Functional Consequences of Extreme Adaptations of the Trophic Apparatus in Craniates,” organized by Dominique Adriaens and Anthony Herrel, at the Eighth International Congress on Vertebrate Morphology, Paris, France, 2007.

<sup>†</sup>Corresponding author; e-mail: bruce\_young@uml.edu.

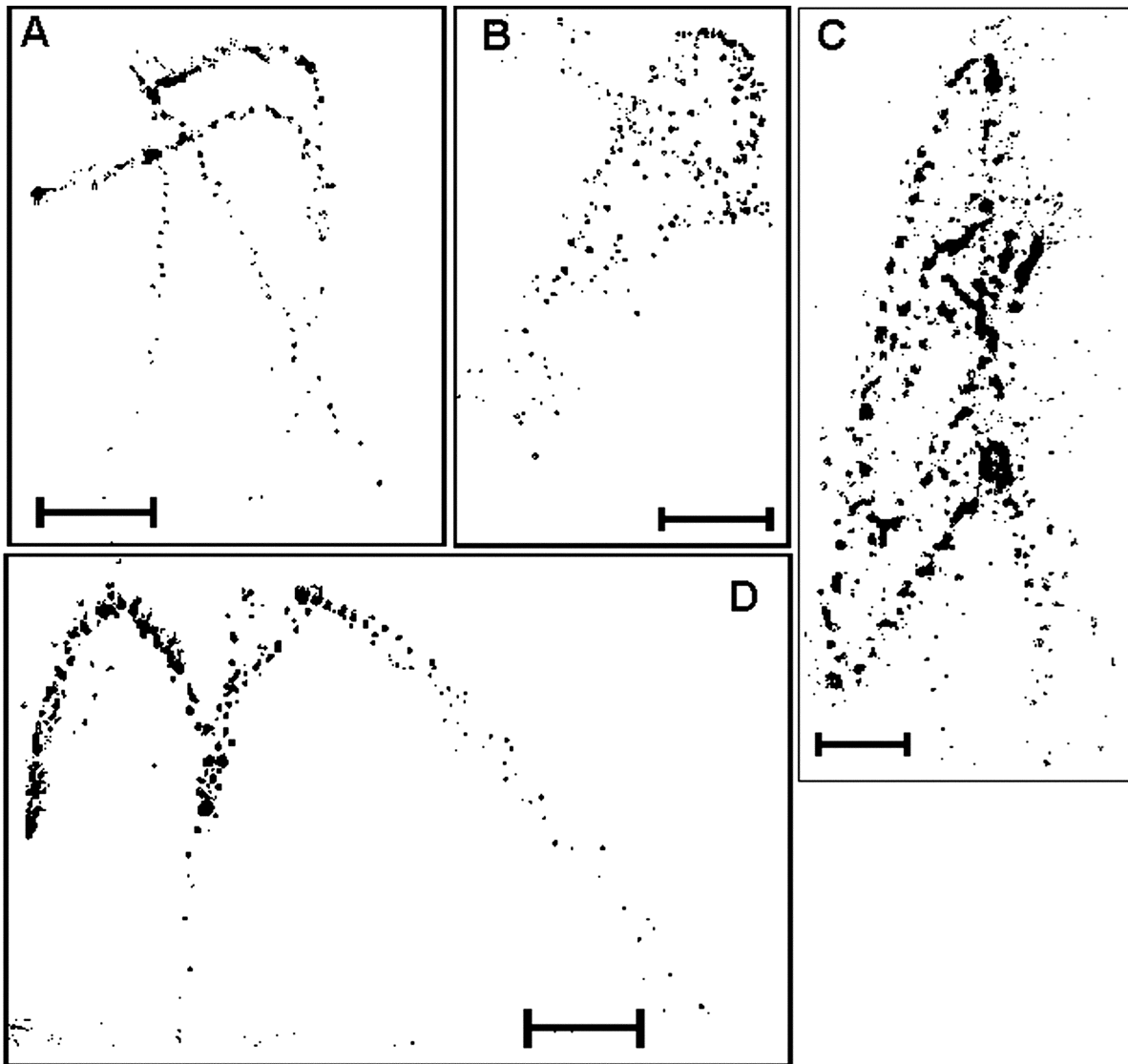


Figure 1. Examples of the variation in the geographic patterns produced by spit venom. Note that while most traces show a distinct venom stream from each fang, in others (B) a more generalized “blob” of venom occurs. Scale bars = 1 cm.

threat when he analogized the evolution of the spitting behavior to the rattling of North American rattlesnakes. Similarly, the recognition that cobras could preferentially direct the spit venom at the eyes formed the underlying rationale for an early series of pathological experiments performed on the corneas of a variety of living animals by Koch and Sachs (1927). It is now well known that the venom spit by cobras can disrupt the cornea, leading to intense pain, temporary or permanent blindness, and even systemic effects (e.g., Warrell and Ormerod 1976; Ismail et al. 1993a, 1993b). The relative accuracy of the cobra, in terms of being able to expel venom onto the surface of the cornea, is less well known.

Bogert (1943) repeats a variety of distances over which cobras are said to be able to spit (including Ditmars’s [1931] claim of 12 ft), and Rasmussen et al. (1995) provide effective spitting ranges for the species they examined. None of these studies

documented the accuracy of the spit. To date, the only study to quantify the relative accuracy of the spit is that of Westhoff et al. (2005), who recorded the distribution of spit venom on the eyes and face of real and photographic targets. In this study, they found that *Naja nigricollis* hit at least one of the target’s eyes in 80% of the trials, whereas *Naja pallida* hit at least one eye in 100% of the trials (trials were conducted at a distance of 60 cm). While this study showed that these species can be highly accurate at hitting the eye, the methodology employed did not allow discrimination between specifically targeting the eye or targeting the region of the face around the eyes. Other studies have suggested that other species of snakes are capable of discriminating the eyes of a target (e.g., Herzog and Bern 1992), although the exact sensory cues involved remain unknown.

One factor complicating any analysis of spitting accuracy is

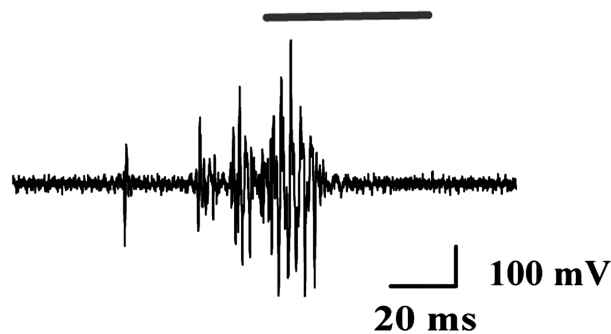


Figure 2. Raw electromyographic trace from the adductor mandibulae externus superficialis (AMES). Note that the onset of activity in the AMES occurs shortly before the venom expulsion (*bar*).

the fact that the venom does not strike the target in a single discrete point but rather is distributed (in some cases widely) over the target. The venom expelled by spitting cobras tends to produce geometric patterns on the target surface (Young et al. 2004; Westhoff et al. 2005); these patterns are highly variable even between successive spits from the same individual (Young and O'Shea 2005). These geometric patterns are most evident in species such as *N. pallida*, where the venom is spit under considerable pressure and the venom from each fang typically forms parallel but distinct planar distributions; in taxa such as *Hemachatus* or *Naja sputatrix*, in which the venom is expelled more as a mist or weak spray, the geometric patterns are less distinctive even though the variation in planar distribution of venom is as high (Rasmussen et al. 1995).

Our study was intended to explore the bases for the geometric patterns of venom dispersal. In particular, we sought to determine whether these venom-dispersal patterns were simply an artifact of the physics of venom expulsion or whether they were actively produced by the cobra. If the spatial distribution of venom is actively controlled by the cobra, questions of relative accuracy or targeting become far more complex.

## Material and Methods

### Live Animals

Adult long-term captive specimens of the red spitting cobra (*Naja pallida*,  $n = 4$ , snout-vent length [SVL] = 120–185 cm), the black-neck spitting cobra (*Naja nigricollis*,  $n = 5$ , SVL = 140–165 cm), and the black-and-white spitting cobra (*Naja siamensis*,  $n = 2$ , SVL = 95 and 115 cm) were used in this study. These animals were maintained at 27°–30°C, with a 12 : 12 light cycle, water ad lib., and a diet of prekilled rodents. All experimental protocols were according to the *Principles of Animal Care*, National Institutes of Health (NIH) publication 86-23, revised 1985. The experimental work was conducted under University of Bonn approval 50.203.2-BN, issued July 2006.

### Spit Patterns

Plastic or glass sheets were positioned between the cobra and the target. The spit venom was caught on these sheets, which were lightly dusted with Rhodamine B (Kremer Pigmente) to enhance the visibility of the (otherwise clear) venom. Venom-distribution patterns were then photographed.

### Morphology of the Fang of Spitting Cobras

The sagittal plane of the fang and venom canal was exposed by grinding the lateral surface of the tooth with 400-grit abrasive paper (Frost 1958). The fang was then mounted, sputter-coated with gold, and examined using a Leo 1450 SEM (Leica, Nensheim, Germany) at 15 kV. A second fang was examined using a Skyscan 1072 (Kontich, Belgium) computer tomography (CT) scanner at 7  $\mu\text{m}/\text{pixel}$  resolution. Reconstruction was done with Skyscan's Nrecon software (using the Feldkamp reconstruction algorithm), and the three-dimensional model was built with Amira.

### Functional Morphology

Individual specimens were anesthetized through exposure to Isoflurane. Hypodermic needles were used to implant bipolar electromyographic (EMG) leads (fabricated from 0.05-mm stainless steel wire with nylon insulation; California Fine Wire, Grover Beach, CA) into the adductor mandibulae externus superficialis (AMES; the compressor of the venom gland), the cervical portion of the semispinalis (responsible for dorsal rotation of the head about the neck), and the cervical portion of the longissimus (responsible for lateral rotation of the head about the neck). A tether of silk suture (1-gauge) was attached to the dorsal surface of the cobra's neck, and the EMG leads were attached to the tether with rubber cement. The EMG

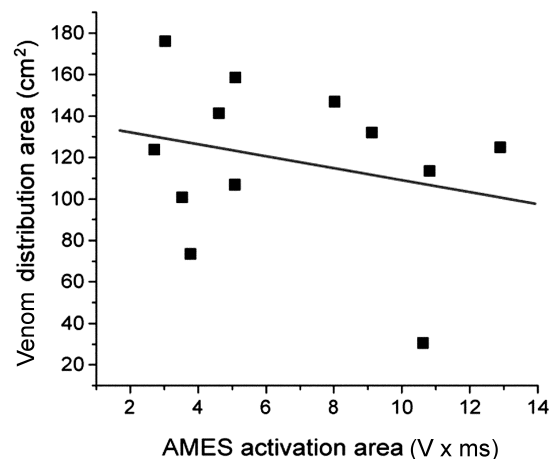


Figure 3. Relationship between the area under the rectified electromyographic trace for the adductor mandibulae externus superficialis (AMES) and the venom-distribution area (measured as an ovoid). The line is the calculated best fit and is not significantly different from a slope of 0.

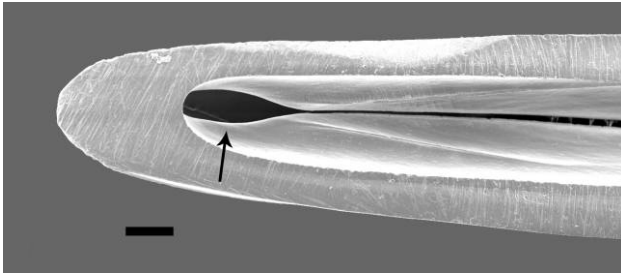


Figure 4. Scanning electron micrograph of a parasagittal section through the fang of *Naja pallida*. The exit orifice of the fang is distinct (arrow), and there is no evidence of any rifling in the venom canal leading to the exit orifice. Scale bar = 1 mm.

signals were amplified using digital oscilloscopes (DL1300A, Yokogawa) before coupling to an A/D converter (Power 1401, Cambridge Electronic Design, Cambridge). Data were recorded at 20 kHz using Spike2 (ver. 5.14) from Cambridge Electronic Design.

As the cobra recovered from anesthesia, it was transferred to a 52-cm-high  $\times$  45-cm-wide  $\times$  60-cm-deep filming cage. A mirror suspended at 45° to the floor of the filming cage provided simultaneous lateral and dorsal views of the cobra; 2-cm filming grids attached to the floor and side wall of the cage facilitated later quantification. The movements of the cobra were simultaneously recorded with three different video systems: (1) standard 30-fps video with cameras positioned to document the distance between the cobra and the target; (2) a high-speed digital video camera (Fastex Imaging, San Diego, CA) filming at 500 fps and positioned to record the lateral and dorsal movements of the cobra; and (3) a high-speed digital video camera (Star, LaVision) filming at 1,000 fps and positioned to record the venom stream in the air. The EMG and kinematic records were synchronized using a 1-Hz 100-ms-duration voltage pulse from the data acquisition system to a 5-mW LED red light laser (TIM 203, BLV Electronic) positioned so that the laser flashed into the filming cage at a location visible to all three video systems.

The video records were quantified using ImageJ (NIH). The angle tool of ImageJ was used to quantify both dorsal-ventral (measured from the top of the braincase to the background grid) and lateral (measured from the parasagittal midline of the skull to the background grid) rotations; for this study, we could ignore how much (if any) of these rotational displacements occurred within the vertebral column rather than strictly between the skull and atlas. The EMG data were quantified using a combination of Spike2 and EXCEL spreadsheets. Seven of the specimens (three *N. pallida* and four *N. nigricollis*) were used for EMG analysis; only kinematic data were recorded from the other specimens.

## Results

### Venom Distribution

When treated with Rhodamine B, the spit-venom droplets are easily visualized. Venom spit by *Naja pallida* typically appears

as two parallel streams, one from each functional fang (Fig. 1). These venom streams vary considerably in their horizontal and vertical extent but are almost all characterized by complex overlapping geometric shapes. In some cases, the overlap of the venom streams is so extensive that the individual streams are difficult to distinguish, with the venom distribution appearing more as a reasonably continuous field of venom (Fig. 1B). During the functional trials, the distance between the cobra and the target was  $58 \pm 1.9$  cm (mean  $\pm$  SE;  $n = 78$ ). The venom spit during these trials was captured on acetate sheets attached to the face shield worn by the target; these sheets were evaluated using very conservative criteria to ensure that all spit venom was clearly represented on the sheet. Only 17 sheets were used for the final analysis. These 17 sheets had a horizontal distribution of  $12.2 \pm 2.4$  cm and a vertical distribution of  $10.7 \pm 1.7$  cm; when we treated these distributions as ovoids, the total venom area was  $113.6 \pm 29.6$  cm<sup>2</sup>. The distance between the snake and the target had almost no relationship to the area covered by the spit venom ( $t = 1.21$ ,  $P = 0.25$ ,  $r^2 = 0.09$ ,  $n = 16$ ).

### Venom Propulsion

The onset of the spit was defined as the first appearance of venom exiting the fang. Forty seven spits were quantified from the high-speed digital video records; these spits had a duration of  $40.3 \pm 1.4$  ms. With the laser integration, we could plot the temporal profile of the spit onto the EMG record from the AMES, the muscle responsible for venom propulsion, with a temporal resolution of 2 ms (Fig. 2). The rectified EMG signals from the AMES were quantified from 33 trials. These signals had a duration of  $50.8 \pm 2.7$  ms; the percent duration to peak amplitude was  $38.3\% \pm 4.1\%$ , and the area under the rectified signal was  $6.8 \pm 0.7$  V  $\times$  ms. The duration from the onset of activity in the AMES to the onset of spitting was  $21.2 \pm 1.5$  ms ( $n = 26$ ).

Thirteen trials yielded both EMG signals from the AMES and spit-distribution patterns that were quantifiable. Linear regression was used to explore the relationship between venom-distribution area and the duration, the area under the rectified curve (Fig. 3), and the spike amplitude of the AMES. None of the regression coefficients was statistically significant (using a cutoff value of  $P = 0.05$ ). The best relationship was found

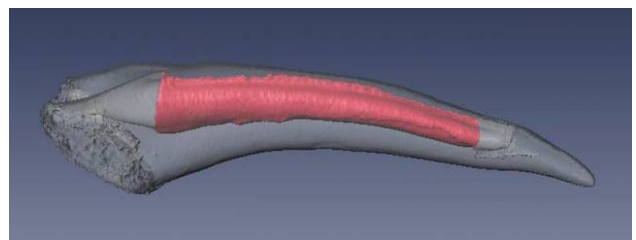


Figure 5. Reconstruction of the venom canal (pink) in the fang of *Naja pallida* using computer tomography (CT). None of the CT images revealed any evidence of rifling on the surface of the venom canal.

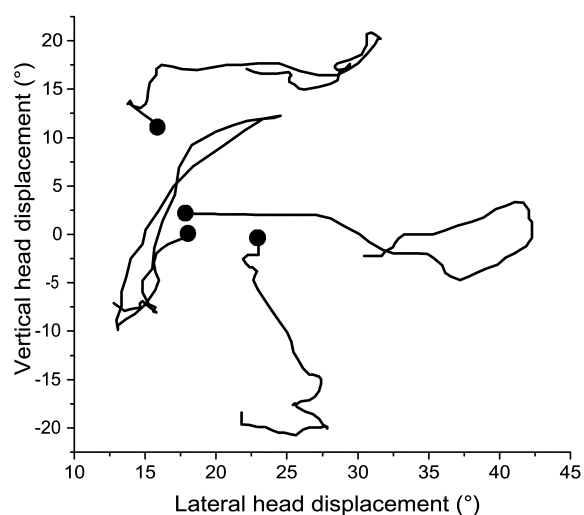


Figure 6. Angular displacement of the cobra's head during spitting. Note the variation in the direction, magnitude, and overall pattern of the cephalic movements; each cephalic displacement includes at least one reversal of direction. Circles are the start of displacement.

between spit-distribution area and the amplitude of the EMG signals from the AMES, but this comparison was far from significant ( $t = -1.09$ ,  $P = 0.30$ ,  $r^2 = 0.11$ ,  $n = 12$ ).

#### Fang Morphology

Scanning electron micrographs (SEMs) of sagittal views of the fang and venom canal revealed the exit orifice (Fig. 4) as well as the immediately adjacent nearly right-angle bend in the venom canal that is one of the key features of venom spitting (Bogert 1943; Wüster and Thorpe 1992). The majority of the length of the venom canal's inner surface is relatively smooth and devoid of grooves or other surface features that could direct the flow of the venom. Low, narrow ridges were present superiorly on either side of the exit orifice, but these extend for less than 20% of the length of the venom canal. The inner contours of the venom canal were further examined using CT scanning, which enabled both a reconstruction of the venom canal and examination of isolated cross sections (Fig. 5). The images generated by the CT scan also showed no indication of ridges or grooves on the inner surface of the venom canal other than the low ridges adjacent to the exit orifice.

#### Cephalic Kinematics during Spitting

During every spitting trial, the cobra made rapid angular movements of its head while expelling venom. These rotations of the head occurred in both the horizontal and the vertical planes, and the resulting patterns of cephalic displacement were highly variable, even between successive spits from the same specimen (Fig. 6). While the cobras were spitting, their heads rotated in the vertical plane through a range of  $12.0^\circ \pm 1.2^\circ$  ( $n = 28$ ) and in the horizontal plane through a range of  $9.7^\circ \pm 1.1^\circ$  ( $n = 28$ ). These ranges of movement do not reflect the total move-

ment of the cobra's head during spitting, because in almost every case, the cobra reversed the direction of these cephalic rotations at least once while spitting. The number of cephalic direction changes while spitting was  $2.6 \pm 1.2$ , which resulted in the more complex geometric patterns when the cranial displacements were plotted in two dimensions (Fig. 6).

The EMG records from the axial muscles also reflect these changing directions in the rotation of the head about the neck. EMG data were gathered only from muscles working in one direction in each plane (e.g., the semispinalis, which is a dorsal rotator of the head, but not from any of the hypaxial muscles that could produce ventral rotation). The activity records we obtained were characteristically pulsatile (Fig. 7), with periods of high-amplitude activity interspersed with periods of lower-level activity or no activity at all. Presumably these interspersed periods reflect when the antagonistic muscle is moving the head in the direction opposite to that produced by the implanted muscle.

Electrical activity within the axial muscles began before the onset of spitting: for semispinalis, the offset was  $48.6 \pm 4.9$  ms ( $n = 24$ ), and for longissimus, the offset was  $40.6 \pm 7.8$  ms ( $n = 13$ ). From the onset of electrical activity to the termination of the spit, but excluding any gaps of presumed antagonistic activity, the duration of activity in the semispinalis was  $45.4 \pm 3.6$  ms, and in the longissimus it was  $61.2 \pm 9.5$  ms. Between the onset of EMG activity and the termination of the spit, and with the same recognition criteria, there were  $2.4 \pm 0.13$  EMG bursts within the semispinalis and  $1.5 \pm 0.19$  EMG bursts within the longissimus, a difference that proved significant ( $t = -5.36$ ,  $P < 0.001$ ). The longest EMG burst recorded from the semispinalis between onset of activity and termination of spitting had a duration of  $30.0 \pm 3.09$  ms, a peak amplitude of  $0.29 \pm 0.04$  V, and an area under the curve of  $1.57 \pm 0.14$  V  $\times$  ms; in 79% of the trials recorded from this muscle (19 out of 24), the initial burst had the longest duration. The longest EMG burst recorded from the longissimus between onset of activity and termination of spitting had a duration of  $58.5 \pm 9.2$  ms, a peak amplitude of  $0.45 \pm 0.04$  V, and an area under the curve of  $5.68 \pm 0.84$  V/ms; in 92% of the trials recorded from this muscle (12 out of 13), the initial burst had the longest

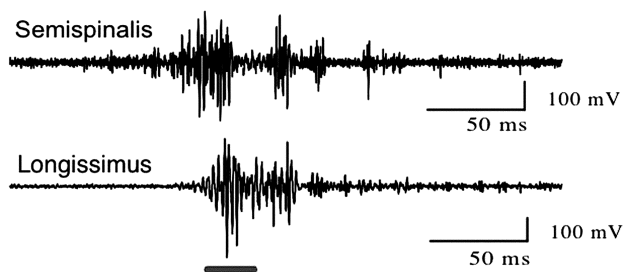


Figure 7. Raw electromyographic traces recorded simultaneously from the semispinalis (dorsal skull rotator) and longissimus (lateral skull rotator) from the same side of the body of a *Naja pallida*. Bar indicates venom expulsion; note that the axial musculature is active before venom expulsion.

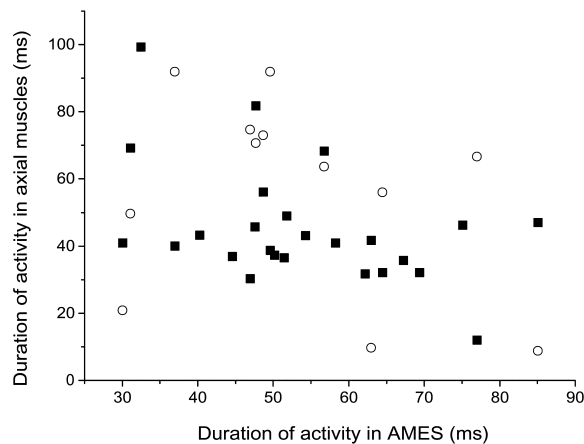


Figure 8. Relationship between the electrical activity in the adductor mandibulae externus superficialis (AMES; X-axis) and axial musculature (Y-axis). Circles = longissimus; squares = semispinalis. Note that there is no significant relationship between the activity patterns of the two muscles.

duration. In all three metrics—duration ( $t = 5.64$ ,  $P < 0.001$ ), peak amplitude ( $t = 3.62$ ,  $P = 0.001$ ), and area under the rectified curve ( $t = 8.76$ ,  $P < 0.001$ )—the activity patterns of these two muscles were significantly different.

The total duration of EMG activity in the axial muscles was compared with the duration of EMG activity in the AMES. Using a Bonferroni-adjusted Pearson correlation coefficient, neither the semispinalis ( $r = -0.45$ ,  $P = 0.15$ ) nor the longissimus ( $r = -0.65$ ,  $P = 0.09$ ) was significantly correlated to the activity of duration in the AMES (Fig. 8).

The rotational head movements preceded the onset of spitting (temporal offset =  $65.2 \pm 4.6$  ms,  $n = 43$ ) and continued after the cessation of spitting, although these postspitting displacements were not analyzed. The range of cephalic head movement (in degrees) was compared with the distribution of spit venom using least squares regression. Both the horizontal ( $t = 2.06$ ,  $P = 0.07$ ,  $n = 11$ ) and the vertical ( $t = 1.97$ ,  $P = 0.08$ ,  $n = 11$ ) movements produced strong ( $r^2 > 0.3$ ) but not significant relationships with venom distribution. The relationship between spit-venom area and the product of the horizontal and vertical ranges of the cobra's head was significant ( $t = 4.15$ ,  $P = 0.002$ ,  $n = 11$ ), with  $r^2 = 0.66$  (Fig. 9).

The temporal pattern of the kinematics and muscle activity associated with venom spitting is presented in Figure 10. The duration of activity within the axial muscles (semispinalis and longissimus) is expressed exclusively of the periods of agonistic activity, which extend the active period of these muscles considerably.

#### Predicted Spit Patterns

Using planar trigonometry, the rotations of the cobra's head during spitting were combined with the distance between the snake and the target (the hypotenuse) during each spitting episode to predict the spatial distribution of the spit venom.

These predictions assumed a constant distance of 2 cm between the right and the left fang, no long-axis rotation of the cobra's head during spitting, and no dispersal of the venom stream. The predicted venom-distribution patterns (Fig. 11) are simpler than but quite similar to the patterns obtained when spit venom is caught on planar sheets (Fig. 1). The predicted spit patterns are based on quantified kinematics of the head during spitting episodes; the actual spit patterns were captured on acetate sheets during some of these trials. Comparing the actual and the predicted spit patterns reveals a good agreement in overall geometry (Fig. 12).

Predicted spit patterns were generated for 31 trials; these patterns had a horizontal range of  $8.3 \pm 0.96$  cm, a vertical range of  $6.4 \pm 0.62$  cm, and (assuming an ovoid distribution) a venom-distribution area of  $44.9 \pm 7.7$  cm<sup>2</sup>. Quantifiable venom distributions were obtained for 10 of these trials; predicted venom distribution is significantly less than the real venom distribution in both the horizontal ( $t = -3.25$ ,  $P = 0.01$ ,  $n = 9$ ) and the vertical ( $t = -5.28$ ,  $P \leq 0.001$ ,  $n = 9$ ) ranges. The total venom areas were not significantly different between the two ( $t = 2.0$ ,  $P = 0.076$ ,  $n = 9$ ), presumably reflecting the range of variation in each data set.

#### Discussion

The spatial patterns of venom distribution documented in this study (Fig. 1) are very similar to those illustrated in previous studies of spitting cobras in the laboratory (Westhoff et al. 2005) or in the field (Young and O'Shea 2005). The same type of geometric patterning is observed whether the venom is collected on a sheet worn or held by a moving target or whether the venom is spit onto a stationary sheet located between the cobra and the target (such as the side of the snake's cage). This relative consistency, coupled with the short duration of the spitting

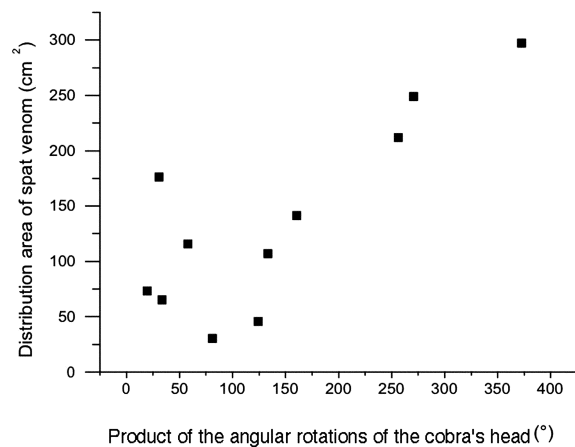


Figure 9. Relationship between cephalic displacements of the cobra's head (the ranges of vertical and horizontal angular displacements were multiplied together using the formula for an ovoid) and venom area (treated as ovoids). There is a significant relationship between the movement of the cobra's head and the spatial distribution of the venom.

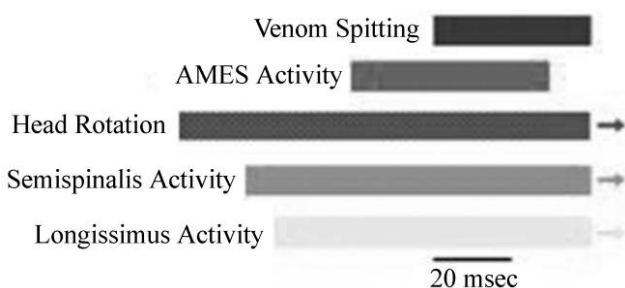


Figure 10. Mean values (as presented in the text) for the temporal pattern among muscle activity patterns and kinematic patterns of venom expulsion and cephalic displacement. Note that the axial muscle activity precedes venom expulsion.

episodes (mean duration of 40.3 ms in this study), strongly suggests that the spatial pattern of the venom was produced by the cobra, not by movements of the target.

Freyvogel and Honegger (1965) generated artificial spits by applying electrical stimulation to the lateral jaw muscles of anesthetized spitting cobras. Young et al. (2004) combined this finding with the repeated observation (e.g., Pitman 1974; Broadley 1983) that the supralabial scalation of spitting cobras displaces during spitting (suggesting an underlying displacement of the maxilla) to produce a more complete model for the functional basis of venom spitting. The model put forth by Young et al. (2004) proposed that venom spitting in cobras utilized the same two key elements found in venom expulsion in viperid snakes: skeletal muscle contraction to pressurize the venom gland and displacement of the fang sheath (Young et al. 2002, 2003; Young and Kardong 2007). The results of our study are consistent with the model put forth by Young et al. (2004) in that the AMES (the muscle that compresses the venom gland) was always active before spitting (mean duration between AMES activity and onset of spitting was 21.2 ms).

Our study was intended to explore the functional basis for the spatial pattern of venom distribution during spitting. The role of the AMES in propelling the venom through the venom-delivery system suggests one hypothesis for spatial patterning: could differential contractile activity within the AMES lead to differential flow of venom through the venom-delivery system and, ultimately, to differential spatial patterning of the spit venom? There are conceptual difficulties with this hypothesis, namely, how changes in pressure could lead to differences in dispersal patterns such as vertical versus horizontal or parallel tracks versus a “uniform” cloud of venom.

This hypothesis was tested by regressing quantitative metrics from the EMG of the AMES against the venom-dispersal area. None of the regression coefficients was statistically different from 0; all of the quantified metrics revealed little relationship with venom dispersal (Fig. 3). Accordingly, the results of our study reveal no support for the hypothesis that variation in contractile activity within the AMES produces variation in the dispersal pattern of spit venom. Given that venom spitting is a two-stage process, with contraction of the AMES being the first stage (Young et al. 2004), it is difficult to imagine how

activity within the AMES could be strongly related to venom pressure, let alone spatial-dispersal patterns. An earlier experimental manipulation of the venom-delivery system of rattlesnakes found a poor relationship between the EMG signals obtained from the skeletal muscle compressing the venom gland and venom pressure and clear evidence that the second stage of the venom-delivery process (fang-sheath deformation) could influence venom kinematics (Young and Kardong 2007).

If not the AMES, is there any other component of the venom-delivery system that could produce the differential spatial distributions of the spit venom? Discussions of venom spitting by cobras occasionally include reference to special grooves or surface features within the venom canal of the fang (e.g., Branch 1992; Greene 1997). These specializations within the venom canal are equated to the grooves that produce rifling within gun barrels and are thus assumed to influence the fluid mechanics and especially the cohesiveness of the expelled venom. This venom canal rifling led to the second hypothesis for venom-dispersal patterns: are the differential venom-dispersal patterns caused by the internal surface features of the venom canal?

This hypothesis is suspect on both evidentiary and conceptual grounds. We are unaware of any photograph or micrograph showing the purported grooves or surface features of the venom canal from a spitting cobra (or any other snake). Bogert (1943), who was specifically interested in the role of the dentition in spitting, examined and depicted both sagittal and transverse sections through the fangs but made no mention of any structures within the venom canal that could produce a rifling of the venom. Similarly, no such structures were reported by Jackson (2002) in her studies of the development of the fang. From a conceptual perspective, it is unclear how a static groove or ridge in the venom canal could produce the divergent patterns of venom distribution that have been reported even from successive spits from the same snake (e.g., Young and O’Shea 2005). This hypothesis was tested by examining the surface of the venom canal using SEM and CT (Figs. 4, 5). No evidence was found of grooves or ridges that could be related to rifling; therefore, this hypothesis is rejected.

Rapid oscillations of the cobra’s head during venom spitting have been previously described (e.g., Young et al. 2004; Westhoff et al. 2005). These cephalic oscillations, like the spatial-dispersal patterns of venom, typically exhibit complex geometric patterns (Fig. 6). The similarity between these patterns led to the third hypothesis for venom dispersal; namely, the spatial-dispersal patterns of spit venom are produced by the rapid movements of the snake’s head during venom expulsion. Simplistically, in this model, the AMES and venom canal can be envisioned as producing a constant stream of venom, the spatial distribution of which would form a discrete point on a screen and which is dispersed by the movements of the snake’s head.

This hypothesis was tested by examining the relationship between the quantified kinematic movements of the cobra’s head and the quantified spatial-distribution patterns of the spit venom. The total spit-venom area was significantly related to the spatial area defined by the cobra’s head during spitting (Fig.

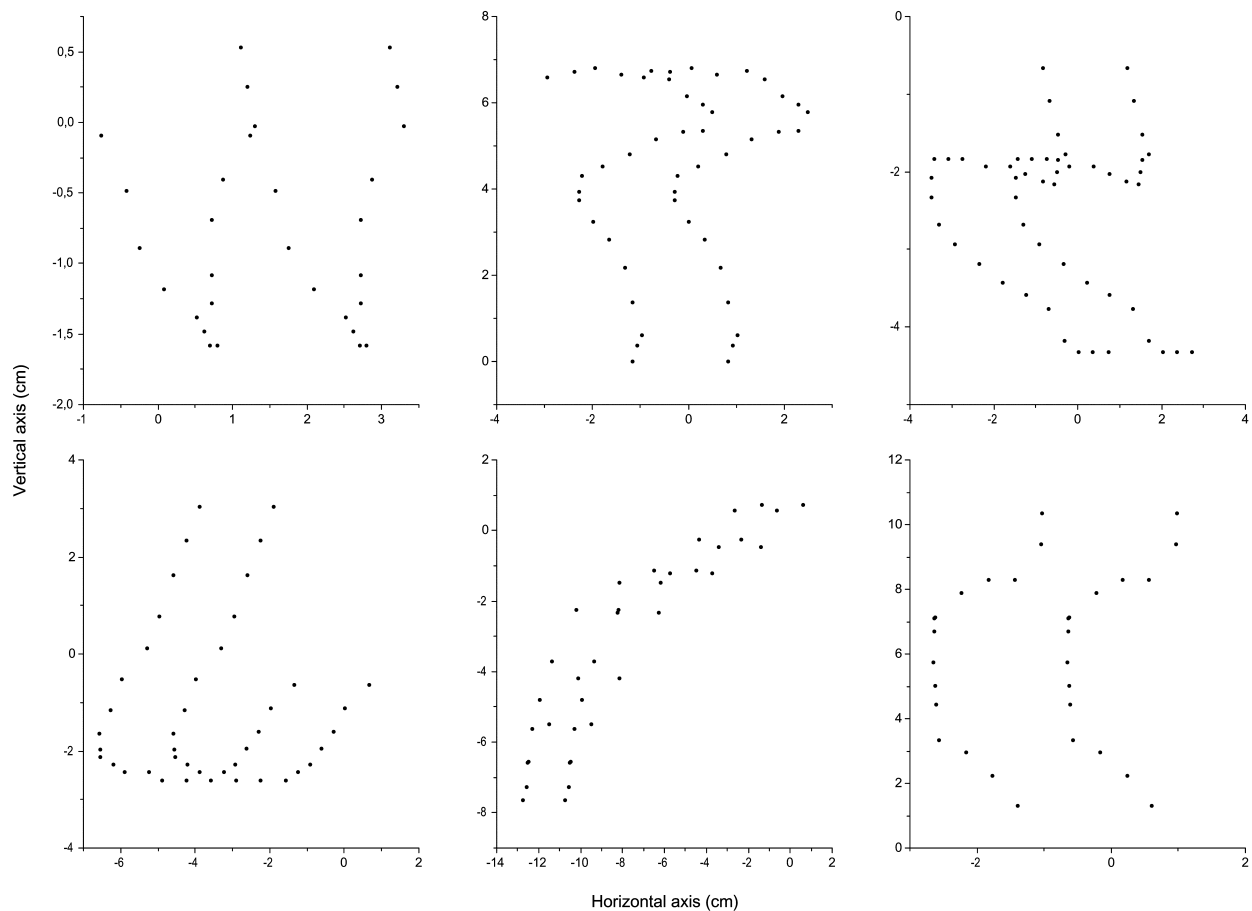


Figure 11. Predicted venom-dispersal patterns based on the angular displacement of the head and the distance from the cobra to the target. All distributions assume a 2-cm distance between fangs and no long-axis rotation of the head. Note the close similarity between these predicted dispersal patterns and the patterns observed from actual venom dispersal (Fig. 1).

9), although here the spatial area was calculated by simply multiplying the two planar values rather than treating the defined area as an ovoid.

As a further test of this hypothesis, we used the quantified cephalic rotations and the distance between the cobra and the target to predict the venom-distribution patterns (Fig. 11). These patterns were both similar to the patterns observed when spit venom is caught (Fig. 1) and in general agreement with the actual spatial patterns from the same trial (Fig. 12). A direct comparison of the predicted and actual venom-distribution areas revealed that the predicted values were significantly less than the actual values for both the horizontal and the vertical spatial range; the total venom area (while still less in the predicted values) was not significantly different. It is not surprising that the predicted values are less than the real venom distribution; the predicted values incorporated three unrealistically restrictive features: (1) the venom leaves the fang as a single point; (2) the venom stream remains completely cohesive while in the air, thus striking the target as a point; and (3) there is no splattering of venom on the target. Relaxing any of these assumptions would have expanded the predicted venom spatial

range and improved the fit between the predicted and the actual data.

The results of this study support the functional model for venom spitting put forth by Young et al. (2004), but they also reveal that the functional specializations for venom spitting in cobras are more complex than detailed in that earlier publication. More specifically, spitting cobras functionally couple the seemingly autonomous cervical axial muscles and the venom-delivery system. The venom-delivery system functions to propel the venom forward while the axial muscles produce rapid oscillations of the head that function to spatially disperse the venom, presumably maximizing the chance that a portion of the spat venom will contact the eye.

During spitting, these two functional complexes seem to perform independently. The only consistent relationship between them is that EMG activity within the axial muscles and the corresponding rotational movements of the head always precede the onset of EMG activity in the AMES and the corresponding onset of spitting (Fig. 10). Neither the quantified kinematic movements of the cobra's head nor the activity patterns within the axial muscles show any significant relationship

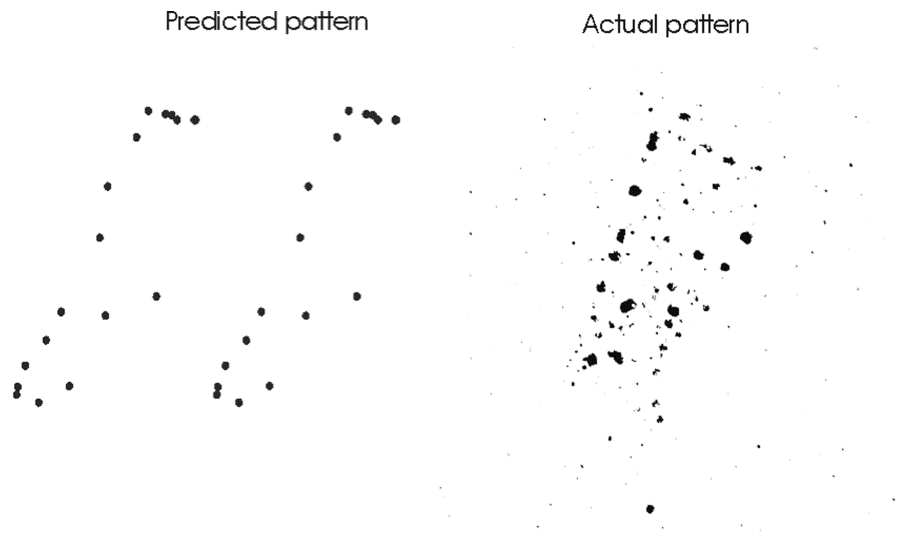


Figure 12. Comparison of a predicted venom-dispersal pattern (prediction based on measured cephalic angular displacements) and the actual venom dispersal from the same trial (image taken from an acetate sheet worn by the target).

to either the duration of the spit or the activity patterns within the AMES (Fig. 8). Similarly, the quantified EMG activity within the AMES has no significant relationship to the spatial dispersal of the venom (Fig. 8).

No previous study has suggested that the cervical axial and venom-delivery system of snakes could function in such an integrated fashion. Kardong and Bels (1998) detailed the kinematics of the rattlesnake strike and suggested that the snakes are incapable of correcting their strike once it has been launched; Young et al. (2001) offered evidence of a rattlesnake correcting an errant strike but agreed that such corrections were quite rare. Virtually all snake strikes require some coordination between the axial and the lateral jaw musculature, and variations in this coordination can lead to very divergent strike behaviors (Cundall et al. 2007).

The duration of venom spitting is less than that of a snake strike, at least the “typical” strike of the species examined in detail to date (see Cundall and Greene 2000 for an excellent review). Despite this, the cephalic rotations characteristic of venom spitting have never been described in other snakes. It would seem intuitive that rapid movements of the head during the strike could “fine-tune” the impact point of the snake’s teeth and/or fangs on the target, thus increasing the efficiency of the strike. The snake strike generally involves a rapid elongation of an initially flexed vertebral column (Kardong and Bels 1998; Cundall and Greene 2000), whereas the rapid movements observed during spitting involve only the head. The large difference in inertia between these two systems could account for some of the absence of rapid rotational movements during the snake strike. Nevertheless, no unique anatomical specializations have been described in the cervical muscles of spitting cobras (Haas 1930; Gasc 1974, 1981), suggesting that other snakes could, provided the appropriate neural stimulation, make the same type of rapid head movements.

The phylogeny of snakes remains contentious, but recent analyses have placed elapids, including the cobras, in one of the most derived groups of snakes (e.g., Slowinski and Keogh 2000; Vidal et al. 2007). Studies of cobra phylogeny have suggested that venom spitting is a recent development within this clade (e.g., Wüster and Broadley 2003). This suggests that the ability to rapidly integrate the cervical musculature and venom-delivery system may be a recent and perhaps unique specialization within this group.

#### Acknowledgments

This work was funded in part by Washburn University, the Kansas Academy of Sciences, the National Institutes of Health (through the Kansas Idea Network of Biomedical Excellence program), and the German Science Foundation. We are indebted to H. Bleckmann for his support and assistance with this research. We thank Stephanie de Pury and Ruben Berthé for the SEM image of the teeth and are grateful to Andreas Peremans from the University of Antwerp for doing the CT reconstruction of the teeth.

#### Literature Cited

- Alexander R.M. 1963. The evolution of the basilisk. *Greece* Rome 10:170–181.
- Barbour T. 1922. Rattlesnakes and spitting snakes. *Copeia* 1922: 36–38.
- Bogert C.M. 1943. Dentitional phenomena in cobras and other elapids with notes on adaptive modification of fangs. *Bull Am Mus Nat Hist* 81:285–360.
- Branch B. 1992. *Everyone’s Guide to Snakes of Southern Africa*:

- Includes Other Reptiles and Amphibians. Central News Agency, Cape Town.
- Broadley D.G. 1972. The herpetology of southern Rhodesia. I. Snakes. *Bull Mus Comp Zool* 120:1–100.
- . 1983. *FitzSimmon's Snakes of Southern Africa*. Delta Books, Johannesburg.
- Cundall D., A. Deufel, and F. Irish. 2007. Feeding in boas and pythons: motor recruitment patterns during striking. Pp. 169–197 in R.W. Henderson and R. Powell, eds. *Biology of the Boas and Pythons*. Eagle Mountain, Eagle Mountain, UT.
- Cundall D. and H. Greene. 2000. Feeding in snakes. Pp. 293–333 in K. Schwenk, ed. *Feeding: Form, Function, and Evolution in Tetrapod Vertebrates*. Academic Press, New York.
- Ditmars R.L. 1931. *Snakes of the World*. Macmillan, New York.
- FitzSimons F.W. 1912. *The Snakes of South Africa: Their Venom and the Treatment of Snake Bite*. Specialty Press, Cape Town.
- Freyvogel T. and C. Honegger 1965. Der "Speiakt" von *Naja nigricollis*. *Acta Trop* 22:289–302.
- Frost H.M. 1958. Preparation of thin undecalcified bone sections by rapid manual method. *Stain Tech* 33:273–277.
- Gadow H. 1901. *Amphibia and Reptiles*. Macmillan, London.
- Gasc J.-P. 1974. L'interprétation fonctionnelle de l'appareil musculo-squelettique de l'axe vertébral chez les serpents (Reptilia). *Mem Mus Natl d'Hist Nat A* 83:1–182.
- . 1981. Axial musculature. Pp. 355–435 in C. Gans and T. Parsons, eds. *Biology of the Reptilia*. Vol. 11. Academic Press, New York.
- Greene H. 1997. *Snakes: The Evolution of Mystery in Nature*. University of California Press, Berkeley.
- Haas G. 1930. Über die Schädelmechanik und die Kiefermuskulatur einiger Proteroglypha. *Zool Jahrb* 52:347–404.
- Herzog H.A. and C. Bern. 1992. Do garter snakes strike at the eyes of predators? *Anim Behav* 44:771–773.
- Ismail M., A.M. al-Bekairi, A.M. el-Bedaiwy, and M.A. Abd-el Salam. 1993a. The ocular effects of spitting cobras. I. The ringhals cobra (*Hemachatus haemachatus*) venom-induced corneal opacification syndrome. *J Toxicol Clin Toxicol* 31: 31–41.
- . 1993b. The ocular effects of spitting cobras. II. Evidence that cardiotoxins are responsible for the corneal opacification syndrome. *J Toxicol Clin Toxicol* 31:45–62.
- Jackson K. 2002. How tubular venom-conducting fangs are formed. *J Morphol* 252:291–297.
- Jones M.D.G. 1900. Can a cobra eject its venom? *J Bombay Nat Hist Soc* 13:376.
- Kardong K. and V. Bels. 1998. Rattlesnake strike behavior: kinematics. *J Exp Biol* 201:837–850.
- Koch M. and W.B. Sachs. 1927. Über zwei giftspeiende Schlangen, *Sepedon haemachates* und *Naia nigricollis*. *Zool Anz* 70: 155–159.
- Laurenti J.N. 1768. *Specimen Medicum, Exhibens Synopsin Reptilium Emendatam cum Experimentis*. Vienna.
- Pitman C. 1974. *A Guide to the Snakes of Uganda*. Wheldon and Wesley, Codicote.
- Rasmussen S., B. Young, and H. Krimm. 1995. On the "spitting" behavior in cobras (Serpentes: Elapidae). *J Zool (Lond)* 237: 27–35.
- Slowinski J. and J. Keogh. 2000. Phylogenetic relationships of elapid snakes based on cytochrome b mtDNA sequence. *Mol Phylogenet Evol* 15:157–164.
- Smith M.A. 1943. *The Fauna of British India, Ceylon and Burma, Including the Whole of the Indo-Chinese Sub-region: Reptilia and Amphibia*. Vol. 3. Serpentes. Taylor & Francis, London.
- Vidal N., A.-S. Delmas, P. David, C. Cruaud, A. Couloux, and S.B. Hedges. 2007. The phylogeny and classification of caenophidian snakes inferred from seven nuclear protein-coding genes. *C R Biol* 330:182–187.
- Visser J. and D.S. Chapman. 1978. *Snakes and Snakebite*. Purnell, Cape Town.
- Wall F. 1921. *Ophidia Taprobanica; or, the Snakes of Ceylon*. Cottle, Colombo.
- Warmington E., ed. 1942. *Pliny: Natural History*. Harvard University Press, Cambridge, MA.
- Warrell D. and L. Ormerod. 1976. Snake venom ophthalmia and blindness caused by the spitting cobra (*Naja nigricollis*) in Nigeria. *Am J Trop Med Hyg* 25:525–529.
- Westhoff G., K. Tzschätzsch, and H. Bleckmann. 2005. The spitting behavior of two species of spitting cobra. *J Comp Physiol A* 191:873–881.
- Wüster W. and D. Broadley. 2003. A new species of spitting cobra (*Naja*) from north-eastern Africa (Serpentes: Elapidae). *J Zool (Lond)* 259:345–359.
- Wüster W. and R.S. Thorpe. 1992. Dentitional phenomena in cobras revisited: spitting and fang structure in the Asiatic species of *Naja* (Serpentes: Elapidae). *Herpetologica* 48:424–434.
- Young B.A., K. Dunlap, K. Koenig, and M. Singer. 2004. The buccal buckle: the functional morphology of venom spitting in cobras. *J Exp Biol* 207:3483–3494.
- Young B.A. and K.V. Kardong. 2007. Mechanisms controlling venom expulsion in the western diamondback rattlesnake, *Crotalus atrox*. *J Exp Zool* 307:18–27.
- Young B.A., C.E. Lee, and K.M. Daley. 2002. Do snakes meter venom? *Bioscience* 52:1121–1126.
- Young B.A. and M. O'Shea. 2005. Analyses of venom spitting in African cobras (Elapidae: Serpentes). *Afr Zool* 60:71–76.
- Young B.A., M. Phelan, J. Jagers, and N. Nejman. 2001. Kinematic modulation of the strike of the western diamondback rattlesnakes (*Crotalus atrox*). *Hamadryad* 26:316–349.
- Young B.A., M. Phelan, M. Morain, M. Ommundsen, and R. Kurt. 2003. Venom injection in rattlesnakes (*Crotalus*): peripheral resistance and the pressure-balance hypothesis. *Can J Zool* 81:313–320.

Copyright of *Physiological & Biochemical Zoology* is the property of University of Chicago Press and its content may not be copied or emailed to multiple sites or posted to a listserv without the copyright holder's express written permission. However, users may print, download, or email articles for individual use.